Cell Stem Cell
Article

Abnormal Calcium Handling Properties Underlie Familial Hypertrophic Cardiomyopathy Pathology in Patient-Specific Induced Pluripotent Stem Cells

Feng Lan,[1,2,3,12] Andrew S. Lee,[1,2,3,12] Ping Liang,[1,2,3,12] Veronica Sanchez-Freire,[1,2,3] Patricia K. Nguyen,[1] Li Wang,[1,2] Leng Han,[1,2] Michelle Yen,[4] Yongming Wang,[1,2,3] Ning Sun,[1,2] Oscar J. Abilez,[5] Shijun Hu,[1,2,3] Antje D. Ebert,[1,2,3] Enrique G. Navarrete,[2] Chelsey S. Simmons,[9] Matthew Wheeler,[1] Beth Pruitt,[9] Richard Lewis,[4] Yoshinori Yamaguchi,[10] Euan A. Ashley,[1] Donald M. Bers,[11] Robert C. Robbins,[2,6] Michael T. Longaker,[3,8] and Joseph C. Wu[1,2,3,7,*]
[1]Department of Medicine, Division of Cardiology
[2]Stanford Cardiovascular Institute
[3]Institute for Stem Cell Biology and Regenerative Medicine
[4]Department of Molecular and Cellular Physiology
[5]Department of Surgery, Division of Vascular Surgery
[6]Department of Cardiothoracic Surgery
[7]Department of Radiology, Molecular Imaging Program
[8]Department of Surgery, Division of Plastic and Reconstructive Surgery
Stanford University School of Medicine, Stanford, CA 94305, USA
[9]Department of Mechanical Engineering, Stanford University School of Engineering, Stanford, CA 94305, USA
[10]Department of Applied Physics, Osaka University, Osaka 565-0871, Japan
[11]Department of Pharmacology, UC Davis, Davis, CA 95616, USA
[12]These authors contributed equally to this work
*Correspondence: joewu@stanford.edu
http://dx.doi.org/10.1016/j.stem.2012.10.010

SUMMARY

Familial hypertrophic cardiomyopathy (HCM) is a prevalent hereditary cardiac disorder linked to arrhythmia and sudden cardiac death. While the causes of HCM have been identified as genetic mutations in the cardiac sarcomere, the pathways by which sarcomeric mutations engender myocyte hypertrophy and electrophysiological abnormalities are not understood. To elucidate the mechanisms underlying HCM development, we generated patient-specific induced pluripotent stem cell cardiomyocytes (iPSC-CMs) from a ten-member family cohort carrying a hereditary HCM missense mutation (Arg663His) in the *MYH7* gene. Diseased iPSC-CMs recapitulated numerous aspects of the HCM phenotype including cellular enlargement and contractile arrhythmia at the single-cell level. Calcium (Ca^{2+}) imaging indicated dysregulation of Ca^{2+} cycling and elevation in intracellular Ca^{2+} ($[Ca^{2+}]_i$) are central mechanisms for disease pathogenesis. Pharmacological restoration of Ca^{2+} homeostasis prevented development of hypertrophy and electrophysiological irregularities. We anticipate that these findings will help elucidate the mechanisms underlying HCM development and identify novel therapies for the disease.

INTRODUCTION

Hypertrophic cardiomyopathy (HCM) is an autosomal dominant disease of the cardiac sarcomere and is estimated to be the most prevalent hereditary heart condition in the world (Maron et al., 1995; Teare, 1958). Patients with HCM exhibit abnormal thickening of the left ventricular (LV) myocardium in the absence of increased hemodynamic burden and are at heightened risk for clinical complications such as progressive heart failure, arrhythmia, and sudden cardiac death (SCD) (Maron, 2002; Maron et al., 2003). Molecular genetic studies from the past two decades have demonstrated that HCM is caused by mutations in genes encoding for proteins in the cardiac sarcomere (Geisterfer-Lowrance et al., 1990; Seidman and Seidman, 2001). While identification of specific mutations has defined the genetic causes of HCM, the pathways by which sarcomeric mutations lead to myocyte hypertrophy and ventricular arrhythmia are not well understood. Efforts to elucidate the mechanisms underlying development of HCM have yielded conflicting results, paradoxically supporting models of both loss in myosin function and gain in myosin function to explain development of the disease (Arad et al., 2002; Marian et al., 1997; Tyska et al., 2000).

Attempts to resolve these discrepancies have been hampered by difficulties in obtaining human cardiac tissue and the inability to propagate heart samples in culture. To circumvent these hurdles, we generated induced pluripotent stem cell-derived cardiomyocytes (iPSC-CMs) from a family of ten individuals, half of whom carry an autosomal dominant missense mutation on exon 18 of the β-myosin heavy chain gene (*MYH7*) encoding for an Arginine to Histidine substitution at amino acid position 663 (Arg663His). We report here that the generation of patient-specific iPSC-CMs allows for recapitulation of the HCM disease phenotype at the single-cell level and that elevation in intracellular Ca^{2+} ($[Ca^{2+}]_i$) is a central mechanism underlying pathogenesis of the disease. These findings validate iPSC technology as a method to understand how sarcomeric mutations cause the

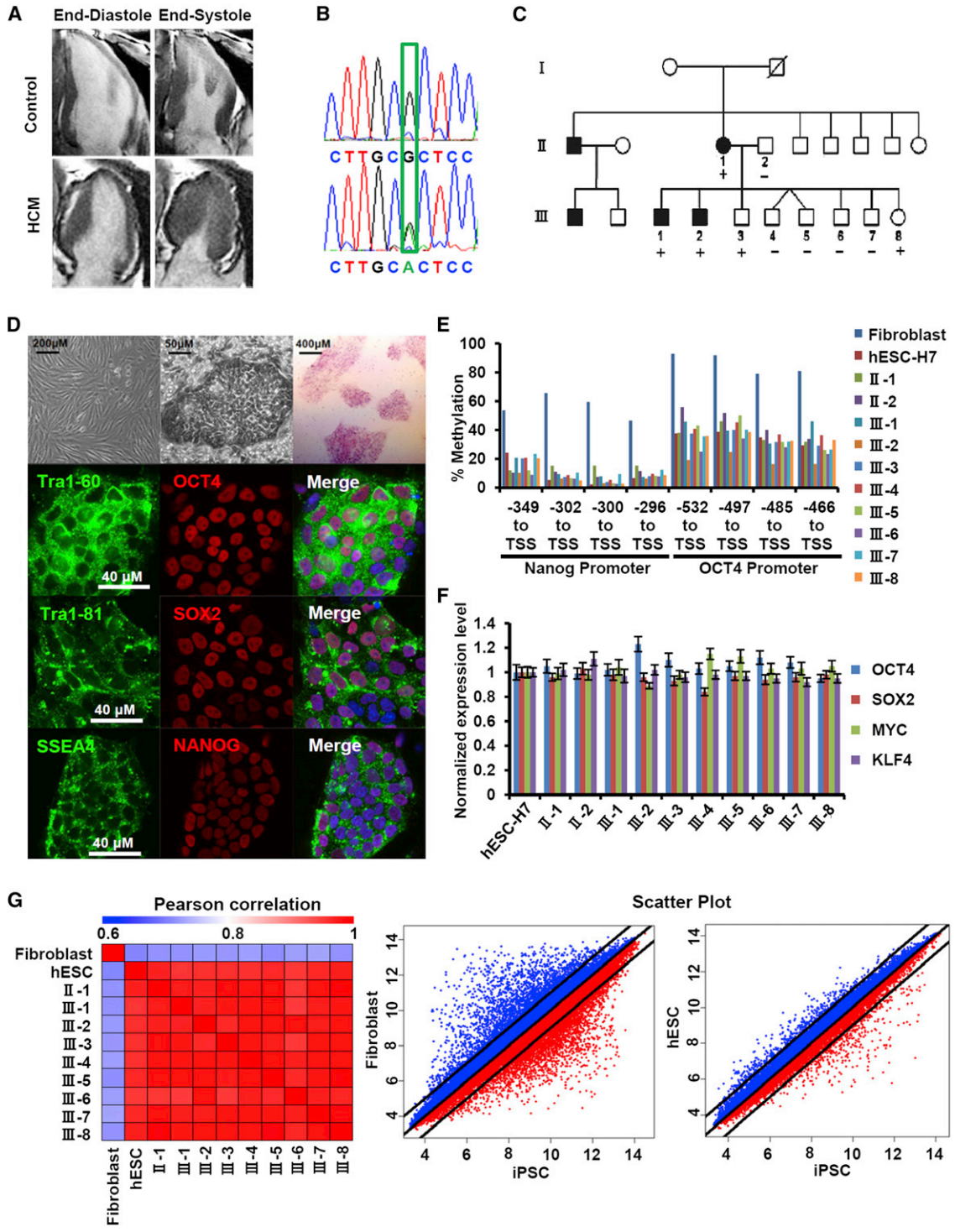

Figure 1. Derivation and Characterization of Patient-Specific iPSCs

(A) Representative long-axis MRI images of the proband and a control matched family member at end systole and end diastole demonstrating asymmetric hypertrophy of the inferior wall. See also Figure S1A and Movie S1.

(B) Confirmation of the Arg663His missense mutation on exon 18 of the *MYH7* gene in HCM patients (II-1, III-1, III-2, III-3, and III-8) by PCR and sequence analysis.

(C) Schematic pedigree of the proband carrying the Arg663His mutation in MYH7 recruited for this study (II-1) as well as her husband (II-2) and eight children (III-1 through III-8). Circles represent female family members and squares represent males. Solid symbols indicate clinical presentation of the HCM phenotype, whereas open symbols represent absence of presentation. "+" and "−" signs underneath family members indicate presence and absence of the Arg663His mutation, respectively. Two individuals (III-3 and III-8) were found to carry the Arg663His mutation but had yet to present the HCM phenotype due to young age. See also Table S1.

(legend continued on next page)

development of HCM and to identify new therapeutic targets for the disease.

RESULTS

Recruitment of HCM Family Cohort and Evaluation of Disease Genotype and Phenotype

A ten-member family cohort that spanned two generations (II and III) was recruited for isolation of dermal fibroblasts. The proband was a 53-year-old African American female patient (II-1) who presented at the hospital with palpitations, shortness of breath, and exertional chest pain. Results from comprehensive testing revealed concentric left ventricular hypertrophy (LVH) with prominent thickening of the inferior septum and inferior wall (Figure 1A and see Figure S1A, Table S1, and Movie S1 available online). To confirm presence of an HCM-causing mutation, we screened the proband's genomic DNA for mutations with a panel of 18 genes associated with HCM including ACTC1, CAV3, GLA, LAMP2, MTTG, MTTI, MTTK, MTTQ, MYBPC3, MYH7, MYL2, MYL3, PRKAG2, TNNC1, TNNI3, TNNT2, TPMI, and TTR. Nucleotide sequence analysis demonstrated a known familial HCM missense mutation on exon 18 of the β-myosin heavy chain (MYH7) gene, which causes an Arginine to Histidine substitution at amino acid position 663 (Arg663His; Figure 1B) (Gruver et al., 1999). Subsequent genetic evaluation of the proband's family revealed that four of her eight children (III-1, III-2, III-3, and III-8; ages 21, 18, 14, and 10) carried the Arg663His mutation (Figure 1C). The proband's family underwent the same comprehensive clinical evaluation, which revealed mild LVH in the two eldest carriers on echocardiography and MRI as well as occasional premature ventricular contractions on ambulatory monitoring. The two younger carriers (III-3 and III-8; ages 14 and 10) had not fully developed the phenotype due to their young age but did exhibit hyperdynamic function by echocardiography (summarized in Table S1). As onset of HCM typically occurs after 18 years of age, these clinical findings were typical for preadolescent and adolescent mutant carriers who later manifest the disease in adulthood. The proband's husband (II-2; age 55) and other four children (III-4, III-5, III-6, and III-7; ages 20, 16, 14, and 13) did not carry the mutation or exhibit any cardiac abnormalities upon examination.

Generation of Patient-Specific iPSCs and Confirmation of Pluripotency

Patient-specific iPSCs were generated from primary fibroblasts of all ten individuals through lentiviral infection with the reprogramming factors *Oct-4*, *Sox-2*, *Klf-4*, and *c-Myc*. A minimum of three distinct lines was generated per patient and assayed for pluripotency through a battery of tests. Established iPSCs exhibited positive immunostaining for the ESC markers SSEA-4, TRA-1-60, TRA-1-81, OCT4, SOX2, NANOG, and alkaline phosphatase, as well as protein expression for the transcription factors OCT4, SOX2, and NANOG (Figure 1D, Figure S1B). Quantitative bisulfite pyrosequencing and quantitative RT-PCR demonstrated hypomethylation of *NANOG* and *OCT4* promoters, activation of endogenous pluripotency transcription factors, and silencing of lentiviral transgenes (Figures 1E and 1F). Microarray analyses comparing whole-genome expression profiles of dermal fibroblasts, iPSCs, and human ESCs (WA09 line) further confirmed successful reprogramming of all cell lines (Figure 1G). Karyotyping demonstrated stable chromosomal integrity in all iPSC lines through passage 30 (Figure S1C). Spontaneous embryoid body (EB) and teratoma formation assays yielded cellular derivatives of all three germ layers in vitro and in vivo, confirming the pluripotent nature of generated iPSCs (Figures S1D–S1F). Restriction enzyme digestion and sequencing verified the presence and absence of the Arg663His mutation in the *MYH7* locus of HCM and control iPSCs, respectively (Figure S1G).

Differentiation of Patient-Specific iPSCs into Cardiomyocytes

Established iPSC lines from all subjects were differentiated into cardiomyocyte lineages (iPSC-CMs) using standard three-dimensional (3D) EB differentiation protocols (Yang et al., 2008). Ten to twenty days after the initiation of differentiation, spontaneously contracting EBs were observed to appear under light microscopy. Immunostaining for cardiac Troponin T indicated that beating EBs from both control and HCM iPSC lines contained cardiomyocyte purities between 60%–80% (Figures S2A and S2B). Beating EBs were seeded on multielectrode array (MEA) probes for evaluation of electrophysiological properties. Both control and HCM iPSC-derived EBs exhibited comparable beat frequencies, field potentials, and upstroke velocities at baseline (Table S2). EBs were subsequently dissociated into single iPSC-CMs and plated on gelatin-coated chamber slides for further analysis. Single dissociated iPSC-CMs from both HCM and control family members maintained spontaneous contraction and exhibited positive staining for sarcomeric proteins such as cardiac troponin T and myosin light chain *(MLC)2a* and *MLC2v* (Figure 2A and Figures S2C and S2D).

iPSC-CMs Carrying the Arg663His Mutation Recapitulate HCM Phenotype In Vitro

After cardiac differentiation and dissociation to single beating cells, diseased and control-matched iPSC-CMs were

(D) Brightfield and immunofluorescence microscopy photographs of patient-specific dermal fibroblasts, representative iPSC colony derived from patient-specific fibroblasts, alkaline phosphatase (AP) staining of pluripotent colonies, and markers of pluripotency including TRA-1-60, OCT4, TRA-1-81, SOX2, SSEA-4, and NANOG. See also Figures S1B–S1G.

(E) Quantitative bisulfite pyrosequencing of the methylation status of Nanog and Oct4 promoter regions in ten patient-specific iPSC lines derived from five family members with HCM (II-1, III-1, III-2, III-3, and III-8) and five control matched family members (II-2, III-4, III-5, III-6, and III-7). Fibroblasts and H7 human ESCs were used as negative and positive controls, respectively.

(F) Ratios of quantitative PCR values for total versus endogenous expression of the Yamanaka factors *OCT4*, *SOX2*, *c-MYC*, and *KLF4* in patient-specific iPSC lines derived from five HCM (II-1, III-1, III-2, III-3, and III-8) and five control (II-2, III-4, III-5, III-6, and III-7) family members. Human ESC from the H7 line was used as controls.

(G) Scatter plots comparing whole genome expression of patient-specific iPSC lines, H7 ESCs, and dermal fibroblasts. Genes with SD greater than 0.2 among all samples (n = 13,044) were selected for Pearson correlation analysis. Error bars represent SEM.

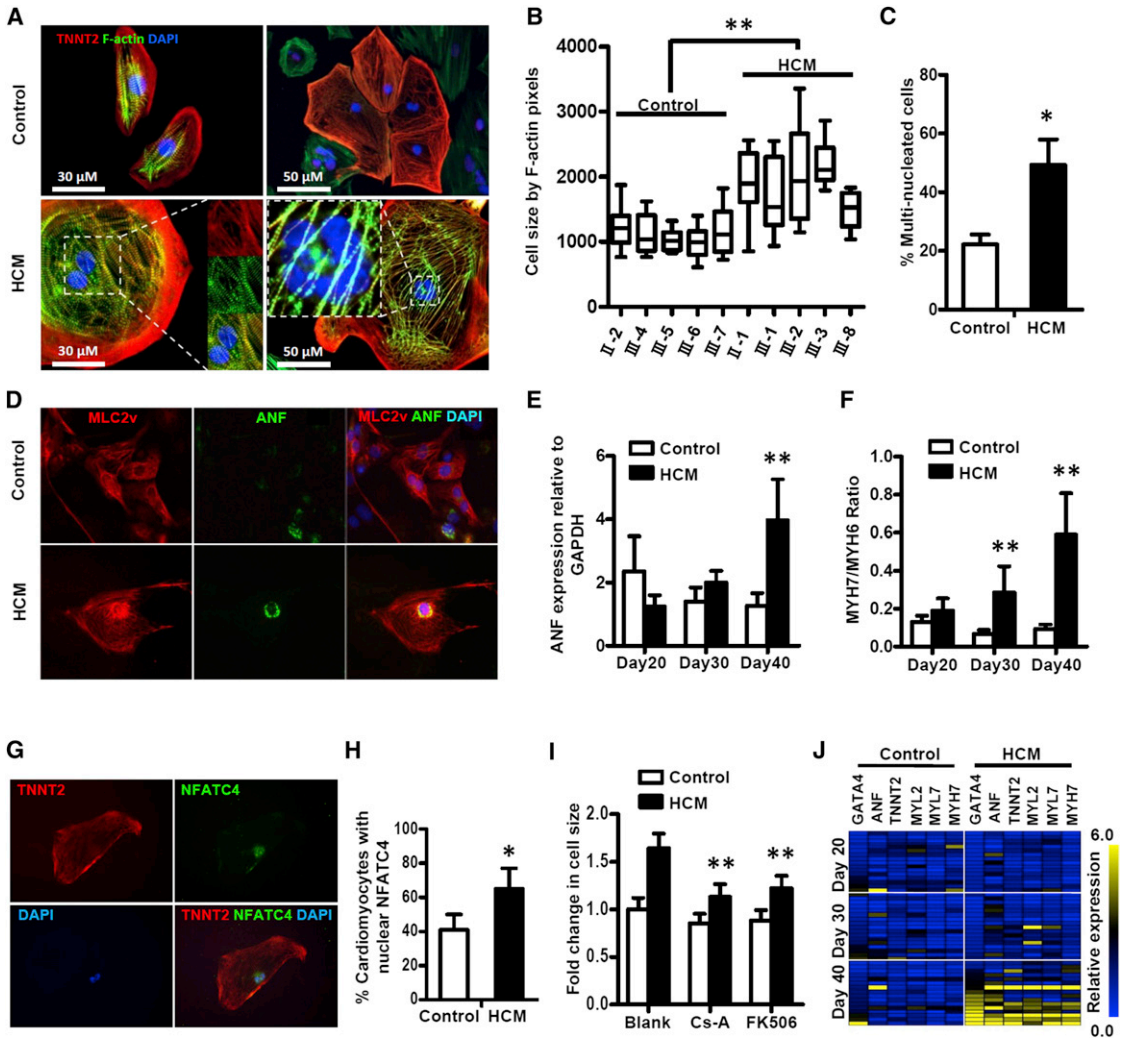

Figure 2. Generation and Characterization of Patient-Specific HCM iPSC-CMs

(A) Representative immunostaining for cardiac troponin T and F-actin demonstrating increased cellular size and multinucleation in HCM iPSC-CMs as compared to control iPSC-CMs. See also Figures S2A–S2D.

(B) Quantification of cell size for five control iPSC-CM lines (II-2, III-4, III-5, III-6, and III-7) (n = 55 per patient line) and five HCM iPSC-CM lines (II-1, III-1, III-2, III-3, and III-8) (n = 59 per patient line) 40 days after induction of cardiac differentiation.

(C) Quantification of multinucleation in control (n = 55, 5 control subject lines) and HCM (n = 59, 5 patient lines) iPSC-CMs.

(D) Representative immunofluorescence staining reveals elevated ANF expression in the *MLC2v*-positive ventricular HCM iPSC-CMs as compared to controls.

(E) Changes in *ANF* gene expression as measured by single-cell quantitative PCR in control and HCM iPSC-CMs at days 20, 30, and 40 after induction of cardiac differentiation (n = 32 per time point, 5 control subject and 5 patient lines).

(F) Quantification of *MYH7*/*MYH6* expression ratio in HCM iPSC-CMs and controls (n = 32 per time point, 5 control subject and 5 patient lines).

(G) Representative immunofluorescence staining images revealing nuclear translocation of NFATC4 in HCM iPSC-CMs.

(H) Percentage of cardiomyocytes exhibiting positive NFATC4 staining in control (n = 187, 5 control subject lines) and HCM (n = 169, 5 patient lines) iPSC-CMs.

(I) Quantification of cell size in control and HCM iPSC-CMs after treatment with calcineurin inhibitors CsA and FK506 for 5 continuous days (n = 50, 5 control subject and 5 patient lines per group). See also Figures S2E–S2I.

(J) Heat map representations of gene expression in single control and HCM iPSC-CMs for genes associated with cardiac hypertrophy at days 20, 30, and 40 after induction of cardiac differentiation. See also Figure S3A. *p < 0.05 HCM versus control, **p < 0.0001 HCM versus control. Error bars represent SEM.

characterized in vitro for recapitulation of the HCM phenotype. Hypertrophic iPSC-CMs exhibited features of HCM such as cellular enlargement and multinucleation beginning in the sixth week after induction of cardiac differentiation (Arad et al., 2002). At day 40 postinduction, HCM iPSC-CMs were noticeably larger (1847 ± 507 pixels; n = 295, 5 patient lines) than control matched iPSC-CMs (1146 ± 355 pixels; n = 265, 5 control subject lines) and exhibited significantly higher frequencies of multinucleation (HCM: 48.3% ± 8.7%; n = 288, 5 patient lines versus control: 22.1% ± 3.4%; n = 275, 5 control subject lines) (Figures 2A–2C). Mutant iPSC-CMs also demonstrated other hallmarks of HCM including expression of atrial natriuretic factor (*ANF*), elevation of β-myosin/α-myosin ratio, calcineurin activation, and nuclear translocation of nuclear factor of activated

T cells (*NFAT*) as detected by immunostaining (Figures 2D–2H, Figures S2E and S2F) (Seidman and Seidman, 2001). Analysis of myofibrils by immunofluorescence microscopy revealed further characteristics of HCM in mutant iPSC-CMs such as increased myofibril content (HCM TNNT2 fluorescence intensity = 7.39 ± 0.53 × 10^5, n = 186, 5 patient lines; control TNNT2 fluorescence intensity = 3.60 ± 0.26 × 10^5, n = 173, 5 control subject lines) and a higher percentage of cells exhibiting disorganized sarcomeres (HCM = 16.5% ± 3.6%, n = 186, 5 patient lines; control = 6.6% ± 1.7%, n = 173, 5 control subject lines) (Figures S2G–S2I).

As calcineurin-NFAT signaling is a key transcriptional activator for induction of hypertrophy in adult cardiomyocytes, we sought to test the importance of this pathway to hypertrophic development in HCM iPSC-CMs (Molkentin et al., 1998). Blockade of calcineurin-NFAT interaction in HCM iPSC-CMs by cyclosporin A (CsA) and FK506 reduced hypertrophy by over 40% (Figure 2I). Specificity of CsA and FK506 to disrupt nuclear translocation of NFAT was confirmed by immunostaining (Figures S2E and S2F). In the absence of inhibition, NFAT-activated mediators of hypertrophy such as *GATA4* and *MEF2C* were found to be significantly upregulated in HCM iPSC-CMs beginning day 40 postinduction of cardiac differentiation but not prior to this point (Figure S3A). Taken together, these results indicate that calcineurin-NFAT signaling plays a central role in the development of the HCM phenotype as caused by the Arg663His mutation.

Single-Cell Gene Expression Profiling Demonstrates Activation of HCM-Associated Genes

Clinical presentation of HCM typically occurs over the course of several decades in affected individuals (Maron, 2002). To investigate the temporal effects of the Arg663His mutation upon HCM development at the cellular level, we assessed the expression of hypertrophic-related genes in single purified iPSC-CMs from both HCM and control patients. Single contracting cardiomyocytes were manually lifted from culture dishes at days 20, 30, and 40 from initiation of differentiation and subjected to single-cell quantitative PCR analysis using a panel of cardiomyocyte-related transcripts (Narsinh et al., 2011b). Beginning at day 40, hypertrophic-related genes such as *GATA4*, *TNNT2*, *MYL2*, and *MYH7* were found to be upregulated in HCM iPSC-CMs (Figure 2J, Figure S3A). No significant increases in expression of HCM-related genes were found prior to this time point.

iPSC-CMs Carrying the Arg663His Mutation Exhibit Electrophysiological and Contractile Arrhythmia at the Single-Cell Level

Arrhythmia is a clinical hallmark of HCM and is responsible for a significant portion of morbidity and mortality associated with the disease including sudden cardiac death (Maron, 2002; Maron et al., 1996). We therefore next examined the electrophysiological properties of iPSC-CMs carrying the Arg663His mutation by whole-cell patch clamping. Both HCM and control iPSC-CMs contained myocyte populations characterized by nodal-like, ventricular-like, and atrial-like electrical waveforms, resting membrane potentials, and velocity upstrokes (Figures S3B–S3G). Capacitance measurements of ventricular-type iPSC-CMs indicated HCM cells (62.5 ± 5.8 pF, n = 20, 5 patient lines) were larger than control counterparts (36.1 ± 3.2 pF, n = 19, 5 control subject lines) (Figure S3H). In the first 4 weeks after induction of differentiation, cells from both groups displayed similar action potential frequencies, peak amplitudes, and resting potentials. However, starting at day 30, a large subfraction (40.4% ± 12.9%; n = 131, 5 patient lines) of HCM myocytes as compared to controls (5.1% ± 7.1%; n = 144, 5 control subject lines) were observed to exhibit arrhythmic waveforms including frequent small depolarizations that resembled delayed afterdepolarizations (DADs) that failed to trigger action potentials and clustered beats (Figures 3A1, 3A2, 3B, and 3C) (De Ferrari et al., 1995).

Time-lapse videos of single beating iPSC-CMs under light microscopy confirmed that electrophysiological deficiencies resulted in contractile arrhythmia. Compared to control iPSC-CMs (1.4% ± 1.9%; n = 68, 5 control subject lines), which had regular beat intervals, HCM iPSC-CMs contained numerous cells (12.4% ± 5.0%; n = 64, 5 patient lines) that beat at irregular frequencies. Analysis of single-cell video recordings by pixel quantification software confirmed the arrhythmic nature of HCM iPSC-CM contraction, as well as hypercontractility of diseased cells as compared to controls (Figures S4A–S4E) (Hossain et al., 2010). Taken together, these findings demonstrate sarcomeric mutations are capable of inducing electrophysiological and contractile arrhythmia at the single-cell level.

Overexpression of the Arg663His Mutation in Normal hESC-CMs Recapitulates Calcium Handling Abnormalities of HCM iPSC-CMs

Calcium (Ca^{2+}) plays a fundamental role in regulation of excitation-contraction coupling and electrophysiological signaling in the heart (Bers, 2008). To investigate the possible mechanisms underlying arrhythmia in myocytes carrying the Arg663His mutation, we next analyzed Ca^{2+} handling properties of iPSC-CMs from control and HCM patients using the fluorescent Ca^{2+} dye Fluo-4 acetoxymethyl ester (AM). Compared to iPSC-CMs derived from healthy individuals, HCM iPSC-CMs demonstrated significant Ca^{2+} transient irregularities such as multiple events possibly related to triggered arrhythmia-like voltage waveforms, which were virtually absent in control cells (Figures 3D and 3E and Figures S4F–S4K). Interestingly, irregular Ca^{2+} transients were observed to occur in HCM iPSC-CMs prior to the onset of cellular hypertrophy, suggesting that abnormal Ca^{2+} handling may be a causal factor for the induction of the hypertrophic phenotype. Because variations inherent to spontaneous contractions can potentially confound Ca^{2+} transients, we subjected HCM and control iPSC-CMs to 1 Hz pacing during line scanning. Consistent with data from spontaneous contraction, abnormal Ca^{2+} transients were found to be common in HCM iPSC-CMs (12.5% ± 4.9%; n = 19, 5 patient lines) and absent in control iPSC-CMs (n = 20, 5 control subject lines) (Figures S4L–S4N and Movie S2). To further ensure that observed deficiencies in electrophysiology and Ca^{2+} regulation were due to the Arg663His mutation, we next overexpressed the mutant form of myosin in human embryonic stem cell-derived cardiomyocytes (hESC-CMs; WA09 line). hESC-CMs overexpressing the Arg663His mutant *MYH7* transcript were found to exhibit similar arrhythmias and abnormal Ca^{2+} transients (Figures 3F–3I).

Previous reports have linked intracellular Ca^{2+} ($[Ca^{2+}]_i$) elevation as a trigger for arrhythmia and cellular hypertrophy (Bers,

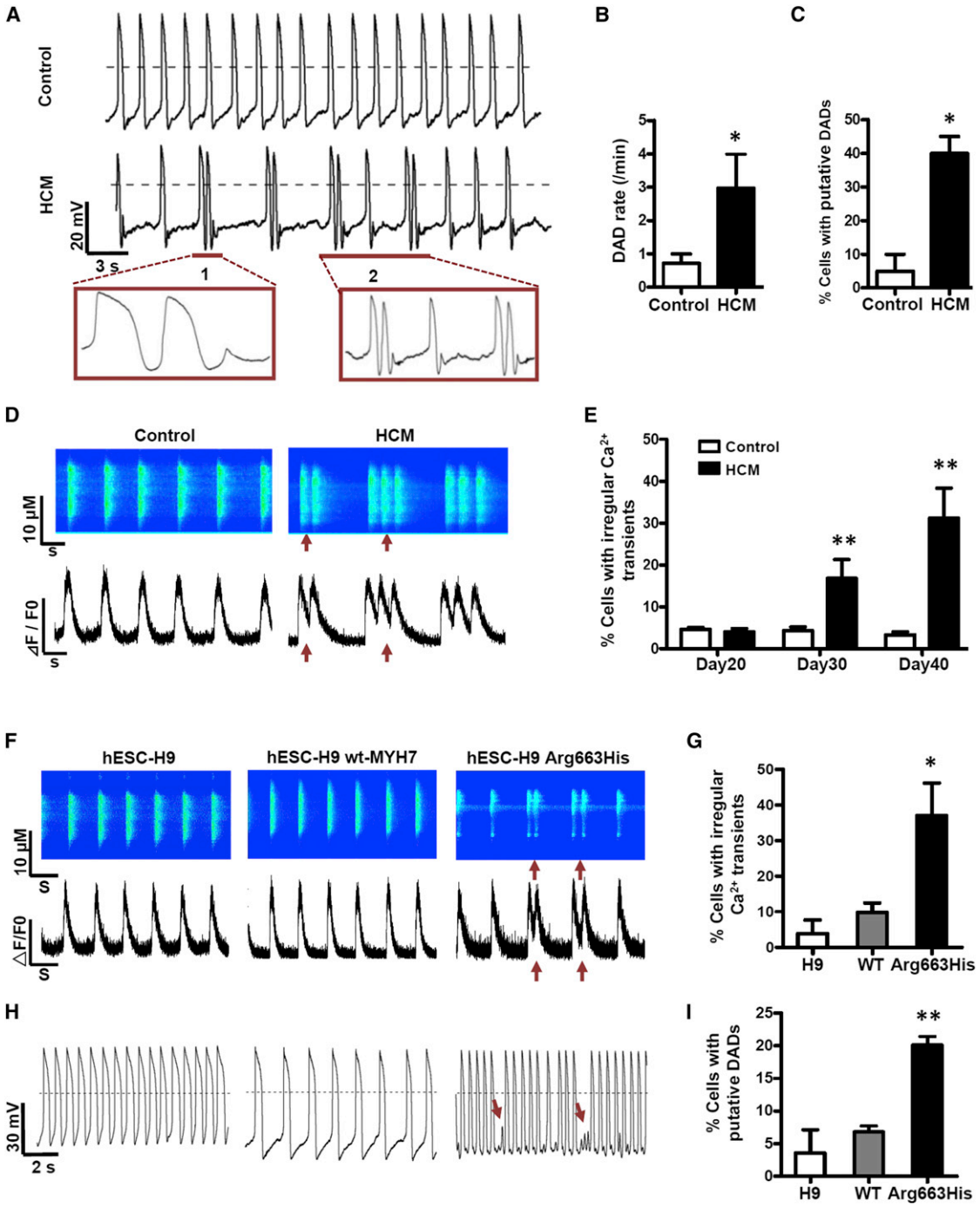

Figure 3. Assessment of Arrhythmia and Irregular Ca^{2+} Regulation in HCM iPSC-CMs

(A) Electrophysiological measurements of spontaneous action potentials in control and HCM iPSC-CMs measured by patch clamp in current-clamp mode. Boxes indicate underlined portions of HCM iPSC-CM waveforms at expanded timescales demonstrating DAD-like arrhythmias. See also Figures S3B–S3H.

(B) Quantification of DAD occurrence in control (n = 144, 5 control subject lines) and HCM (n = 131, 5 patient lines) iPSC-CMs. DAD rate is defined as total DADs/total beats.

(C) Quantification of percentage of control (n = 144, 5 control subject lines) and HCM (n = 131, 5 patient lines) iPSC-CMs exhibiting putative DADs.

(D) Representative line-scan images and spontaneous Ca^{2+} transients in control and HCM iPSC-CMs. Red arrows indicate tachyarrhythmia-like waveforms observed in HCM cells but not control. See also Figures S4A–S4E and Movie S2.

(E) Quantification of percentages for control and HCM iPSC-CMs exhibiting irregular Ca^{2+} transients at days 20, 30, and 40 after induction of cardiac differentiation (n = 50, 5 control subject and 5 patient lines per time point).

(F) Representative line-scan images and spontaneous Ca^{2+} transients for H9 hESC-CMs and hESC-CMs stably transduced with lentivirus driving expression of wild-type *MYH7* or mutant *MYH7* carrying the Arg663His mutation. Red arrowheads indicate irregular Ca^{2+} waveforms.

(legend continued on next page)

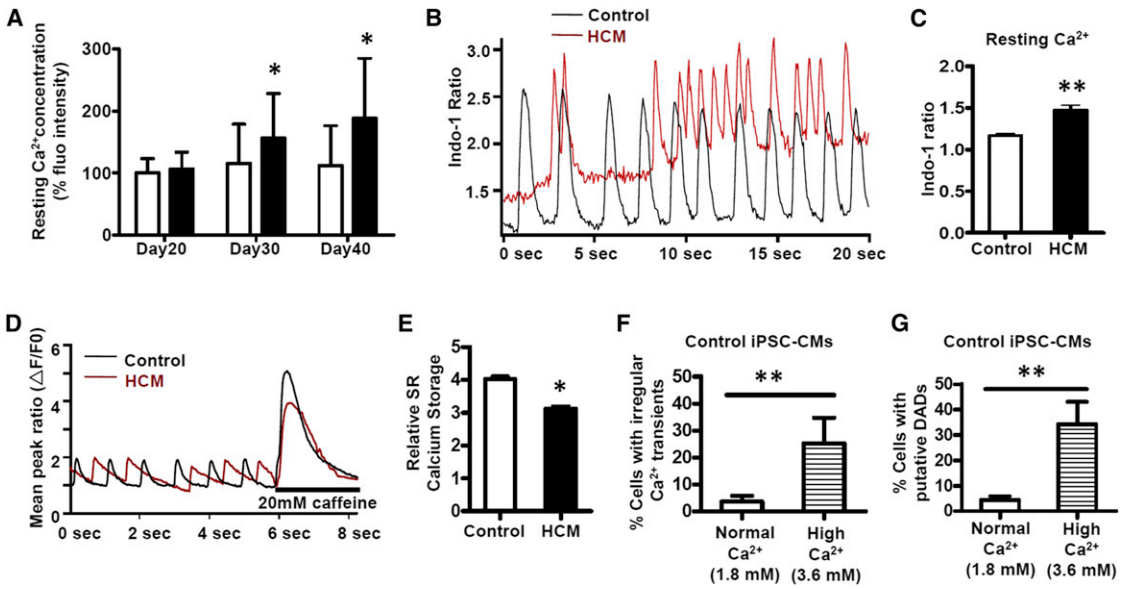

Figure 4. Assessment of Intracellular Ca^{2+} Content in HCM iPSC-CMs

(A) Quantification of baseline Fluo-4 Ca^{2+} dye intensities for control (n = 122, 4 control subject lines) and HCM (n = 105, 4 patient lines) iPSC-CMs. See also Figures S4F–S4N.

(B) Representative Ca^{2+} transients of control and HCM iPSC-CMs using the Indo-1 ratiometric Ca^{2+} dye.

(C) Quantification of resting Ca^{2+} levels by measurement of Indo-1 ratio in control (n = 21, 5 control subject lines) and HCM (n = 30, 5 patient lines) iPSC-CMs.

(D) Representative Ca^{2+} transient traces from control and HCM iPSC-CMs followed by caffeine exposure.

(E) Mean peak amplitudes of ΔF/F0 ratios after caffeine administration representing release of SR Ca^{2+} load for control (n = 36, 5 control subject lines) and HCM (n = 44, 5 patient lines) iPSC-CMs.

(F) Quantification of irregular Ca^{2+} transients for control iPSC-CMs cultured in normal Ca^{2+} media (1.8 mM; n = 280, 5 control subject lines) and high Ca^{2+} media (3.6 mM; n = 67, 5 control subject lines) for 2 hr.

(G) Quantification of DADs for control iPSC-CMs cultured in normal Ca^{2+} media (1.8 mM; n = 144, 5 control subject lines) and high Ca^{2+} media (3.6 mM; n = 32, 5 control subject lines) for 2 hr. *p < 0.05 HCM versus control, **p < 0.01 High Ca^{2+} versus normal Ca^{2+}. Error bars represent SEM.

2008; Molkentin et al., 1998). We therefore further compared $[Ca^{2+}]_i$ in control and diseased iPSC-CMs. Preliminary quantification of $[Ca^{2+}]_i$ by Fluo-4 baseline intensity suggested that $[Ca^{2+}]_i$ was approximately 30% higher in HCM iPSC-CMs (n = 105, 4 patient lines) than control counterparts (n = 122, 4 control subject lines) at day 30 postinduction (Figure 4A). To confirm diastolic $[Ca^{2+}]_i$ differences, we also used the ratiometric Ca^{2+} dye Indo-1 in control and HCM iPSC-CMs. Indo-1 imaging demonstrated that diastolic $[Ca^{2+}]_i$ was higher (26.7% increase in Indo-1 ratio) in iPSC-CMs carrying the Arg663His mutation (n = 30, 5 patient lines) as compared to control cells (n = 21, 5 control subject lines) and that arrhythmic activity was apparent in only the Arg663His myocytes. These findings emphasize a role for irregular Ca^{2+} cycling in the pathogenesis of HCM (Figures 4B and 4C). Measurement of sarcoplasmic reticulum (SR) Ca^{2+} stores further supported findings of elevated $[Ca^{2+}]_i$ in diseased iPSC-CMs, as cytoplasmic retention of Ca^{2+} has been shown to decrease SR Ca^{2+} load by impeding SR Ca^{2+} uptake (Semsarian et al., 2002). HCM and control iPSC-CMs were loaded with Fluo-4 and exposed to caffeine, which induces release of SR Ca^{2+} stores into the cytoplasm. Myocytes carrying the Arg663His mutation were characterized by significantly smaller SR Ca^{2+} release (mean peak ΔF/F0 ratio = 3.12 ± 0.19, n = 44, 5 patient lines) as compared to control iPSC-CMs (mean peak ΔF/F0 ratio = 4.08 + 0.22, n = 36, 5 control subject lines) (Figures 4D and 4E). Finally, to ascertain that irregular calcium transients and arrhythmia were caused by elevated $[Ca^{2+}]_i$, we subjected control iPSC-CMs to culture in high Ca^{2+} (3.6 mM) culture media. As compared to culture under normal Ca^{2+} (1.8 mM) conditions, healthy iPSC-CMs cultured in high Ca^{2+} media were found to develop both irregular Ca^{2+} transients and arrhythmias similar to those observed in HCM iPSC-CMs within 2 hr (Figures 4F and 4G). These findings demonstrate a central role for Ca^{2+} cycling dysfunction and elevated $[Ca^{2+}]_i$ in the pathogenesis of HCM as caused by the Arg663His mutation in *MYH7*.

(G) Quantification of cells exhibiting irregular Ca^{2+} transients in WA09 hESC-CMs, hESC-CMs overexpressing wild-type *MYH7*, and hESC-CMs overexpressing *MYH7* carrying the Arg663His mutation (n = 40, 5 lines per group).

(H) Spontaneous action potentials recorded in current-clamp mode for hESC-CMs, hESC-CMs overexpressing wild-type *MYH7*, and hESC-CMs overexpressing *MYH7* carrying the Arg663His mutation. Red arrowheads indicate DAD-like waveforms.

(I) Quantification of cells exhibiting DAD-like waveforms in hESC-CMs, hESC-CMs stably transduced with lentivirus driving expression of wild-type *MYH7*, or mutant *MYH7* carrying the Arg663His mutation (n = 20, 5 lines per group). Error bars represent SEM.

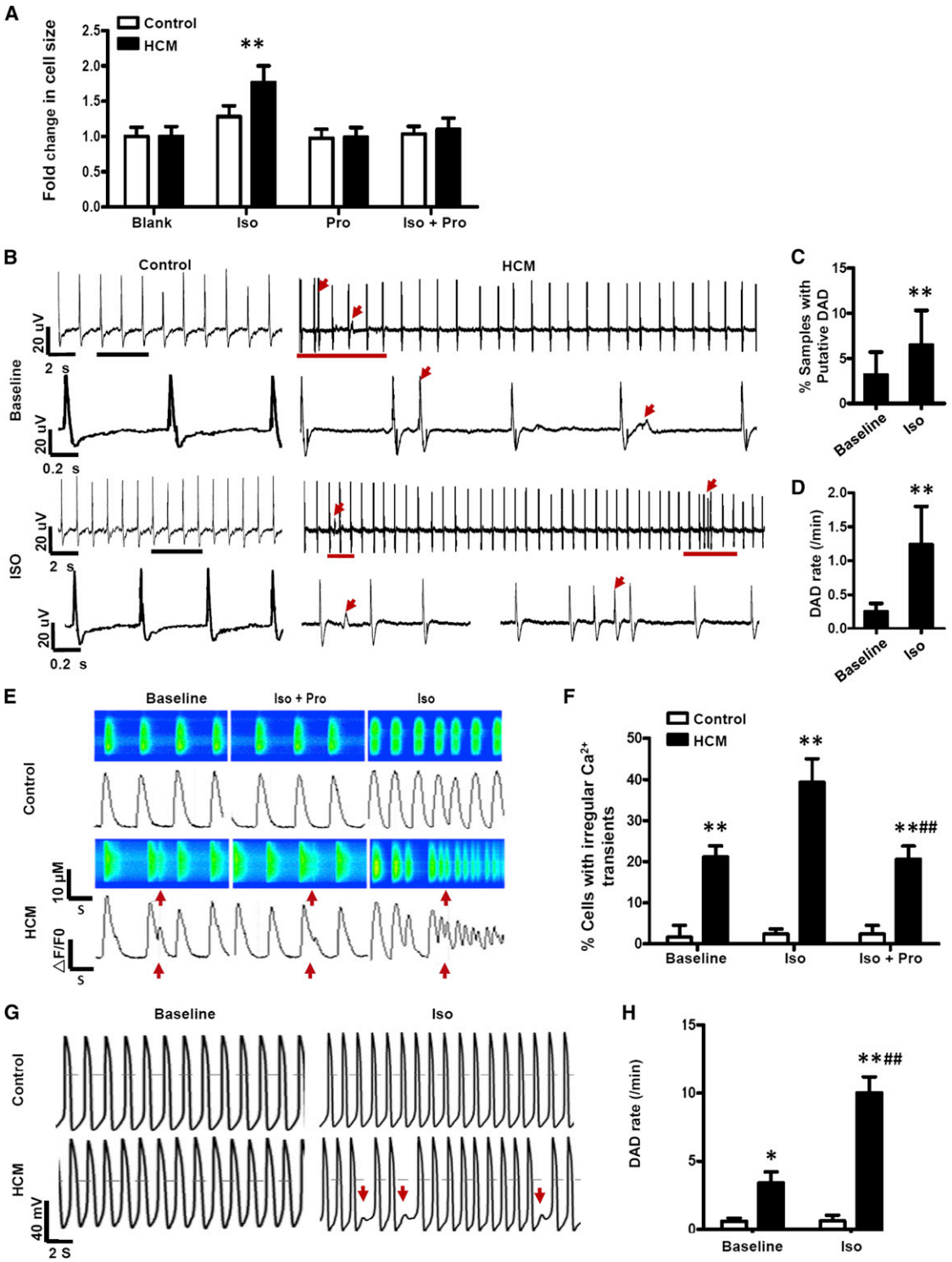

Figure 5. Exacerbation of the HCM Phenotype by Positive Inotropic Stress

(A) Inotropic stimulation of control (n = 50, 5 control subject lines) and HCM (n = 50, 5 patient lines) iPSC-CMs by the β-agonist isoproterenol accelerated presentation of cellular hypertrophy in HCM iPSC-CMs as compared to control counterparts. Coadministration of the β-blocker propranolol prevented catecholamine-induced hypertrophy in HCM iPSC-CMs.

(B) Representative traces of MEA recordings for HCM and control multicellular iPSC-CM preparations. Treatment with 200 nM ISO increased both the beating rate and the prevalence of putative DADs. Red arrowheads indicate putative DAD waveforms. See also Table S2 for baseline MEA measurements.

(C) Quantification of DAD waveforms in multicellular preparations of HCM iPSC-CMs before and after treatment with isoproterenol.

(D) Quantification of putative DAD rate in multicellular preparations of HCM iPSC-CMs before and after treatment with isoproterenol.

(legend continued on next page)

Inotropic Stimulation Exacerbates HCM Phenotype in Diseased iPSC-CMs

Because iPSC-CMs carrying the Arg663His mutation recapitulated numerous aspects of the HCM phenotype in vitro, we hypothesized that our platform could also be used as a screening tool to assess the effect of pharmaceutical drugs upon HCM at the single-cell level. To test the capacity of HCM iPSC-CMs to accurately model pharmaceutical drug response, we first subjected single control and diseased iPSC-CMs to positive inotropic stimulation, a known trigger for myocyte hypertrophy and ventricular tachycardia (Fatkin and Graham, 2002; Knollmann et al., 2003). Patient-specific cardiomyocytes were incubated with β-adrenergic agonist (200 nM isoproterenol) on a daily basis for 5 days beginning 30 days after induction of differentiation. Previously, HCM iPSC-CMs typically did not exhibit cellular hypertrophy until day 40 postinduction (Figure 2B) but were found to increase in cell size by 1.7-fold between day 30 and 35 as compared to control counterparts when treated with isoproterenol (Figure 5A). β-adrenergic stimulation was also found to severely exacerbate presentation of irregular Ca^{2+} transients and arrhythmia in both single and multicellular preparations of HCM iPSC-CMs (Figures 5B–5H). Importantly, coadministration of β-adrenergic blocker (400 nM propranolol) with isoproterenol significantly ameliorated catecholamine-induced exacerbation of hypertrophy, Ca^{2+} handling deficiencies, and arrhythmia.

Treatment of Ca^{2+} Dysregulation Prevents Development of the HCM Phenotype

We next assessed whether pharmaceutical inhibition of Ca^{2+} entry could help prevent HCM phenotype development by treating control and mutant iPSC-CMs with the L-type Ca^{2+} channel blocker verapamil. Compared to control cells, the spontaneous beating rate in HCM iPSC-CMs was relatively resistant to verapamil as detected by MEA dose-response experiments (HCM IC_{50} = 930.61 ± 80.0 nM, 5 patient lines; control IC_{50} = 103.0 ± 6.0 nM, 5 control subject lines), consistent with the elevated $[Ca^{2+}]_i$ in iPSC-CMs carrying the Arg663His mutation (Figures S5A–S5D). Remarkably, continuous addition of verapamil at therapeutic dosages (50–100 nM) to single diseased iPSC-CMs for 10–20 sequential days significantly ameliorated all aspects of the HCM phenotype including myocyte hypertrophy, Ca^{2+}-handling abnormalities, and arrhythmia (Figures 6A–6C). To ensure the pharmaceutical effects observed were specific to Ca^{2+} channel inhibition, we repeated treatment of both single and multicellular preparations of HCM iPSC-CMs with the Ca^{2+} channel blockers nifedipine and diltiazem. As with verapamil, beating rate of HCM iPSC-CMs demonstrated a higher resistance to nifedipine (HCM IC_{50} = 2.3 ± 0.31 μM, n = 8, 5 patient lines) than control cells (control IC_{50} = 0.03 ± 0.005 μM, n = 13, 5 control subject lines). Diltiazem, which is more specific to Ca^{2+} channel inhibition than verapamil, also abolished Ca^{2+}-handling abnormalities and arrhythmia in HCM iPSC-CMs (Figure 6D and Figures S5E and S5F).

Arrhythmic iPSC-CMs Can Be Screened for Potential Pharmaceutical Treatments at the Single-Cell Level

As current pharmaceutical therapy for HCM includes the use of β-blockers and antiarrhythmics in addition to Ca^{2+} channel blockers, we further screened a panel of 12 other drugs used clinically to treat HCM for their potential to ameliorate the HCM phenotype at the single-cell level (Table S3). While verapamil was the only agent found to be capable of preventing cellular hypertrophy, antiarrhythmic drugs that inhibit Na^+ influx such as lidocaine, mexiletine, and ranolazine also demonstrated potential to restore normal beat frequency in HCM iPSC-CMs, possibly through limiting Ca^{2+} entry into the cell by the Na^+/Ca^{2+} exchanger (Figures S6A–S6F, Movie S3). Other antiarrhythmic agents targeting K^+ channels and β-blockers administered in the absence of inotropic stimulation did not have any therapeutic effects in single cells. Altogether, these results strongly implicate imbalances in Ca^{2+} regulation as a central mechanism underlying development of HCM at the cellular level and demonstrate the potential of patient-specific iPSC-CMs as a powerful tool for the identification of novel pharmaceutical agents to treat HCM.

DISCUSSION

The genetic causes of HCM were initially identified several decades ago (Geisterfer-Lowrance et al., 1990). However, the mechanisms by which sarcomeric gene mutations engender the HCM phenotype remain unclear. Modern understanding of HCM is largely based upon transgenic animals engineered to carry human HCM mutations in the murine α-myosin backbone. While these animal models have yielded significant insights into the development of HCM, they also suffer from several limitations that prevent adequate modeling of human cardiac disease. For example, the predominant myosin isoform found in the human cardiac sarcomere is β-myosin, which is largely absent in α-myosin-enriched murine hearts (Fatkin et al., 1999; Lompre et al., 1981). This is especially important in the context of HCM, as β-myosin is the most common causal gene to be mutated for the disease (Seidman and Seidman, 2001). A recent study highlighted the differences in biophysical properties of α- and β-myosin by cloning the same human HCM mutation (R403Q) into both the α-myosin backbone and the β-myosin backbone (Lowey et al., 2008). Remarkably, the same R403Q mutation resulted in completely different functional consequences for myosin contraction depending on whether it was expressed in

(E) Representative Ca^{2+} line scans and waveforms in control and HCM iPSC-CMs after positive inotropic stimulation by isoproterenol. Red arrowheads indicate abnormal Ca^{2+} waveforms.
(F) Quantification of control (n = 50, 5 control subject lines) and HCM (n = 50, 5 patient lines) iPSC-CMs exhibiting irregular Ca^{2+} transients in response to treatment by isoproterenol and coadministration of propranolol.
(G) Electrophysiological measurement of spontaneous action potentials and arrhythmia in control and HCM iPSC-CMs at baseline, followed by positive inotropic stimulation by isoproterenol. Red arrows indicate DAD-like waveforms.
(H) Quantification of DAD rate in control and HCM iPSC-CMs after isoproterenol administration (total DADs/total beats). *$p < 0.05$ HCM versus control, **$p < 0.001$ HCM versus control, $^{\#\#}p < 0.01$ iso + pro versus iso. Error bars represent SEM.

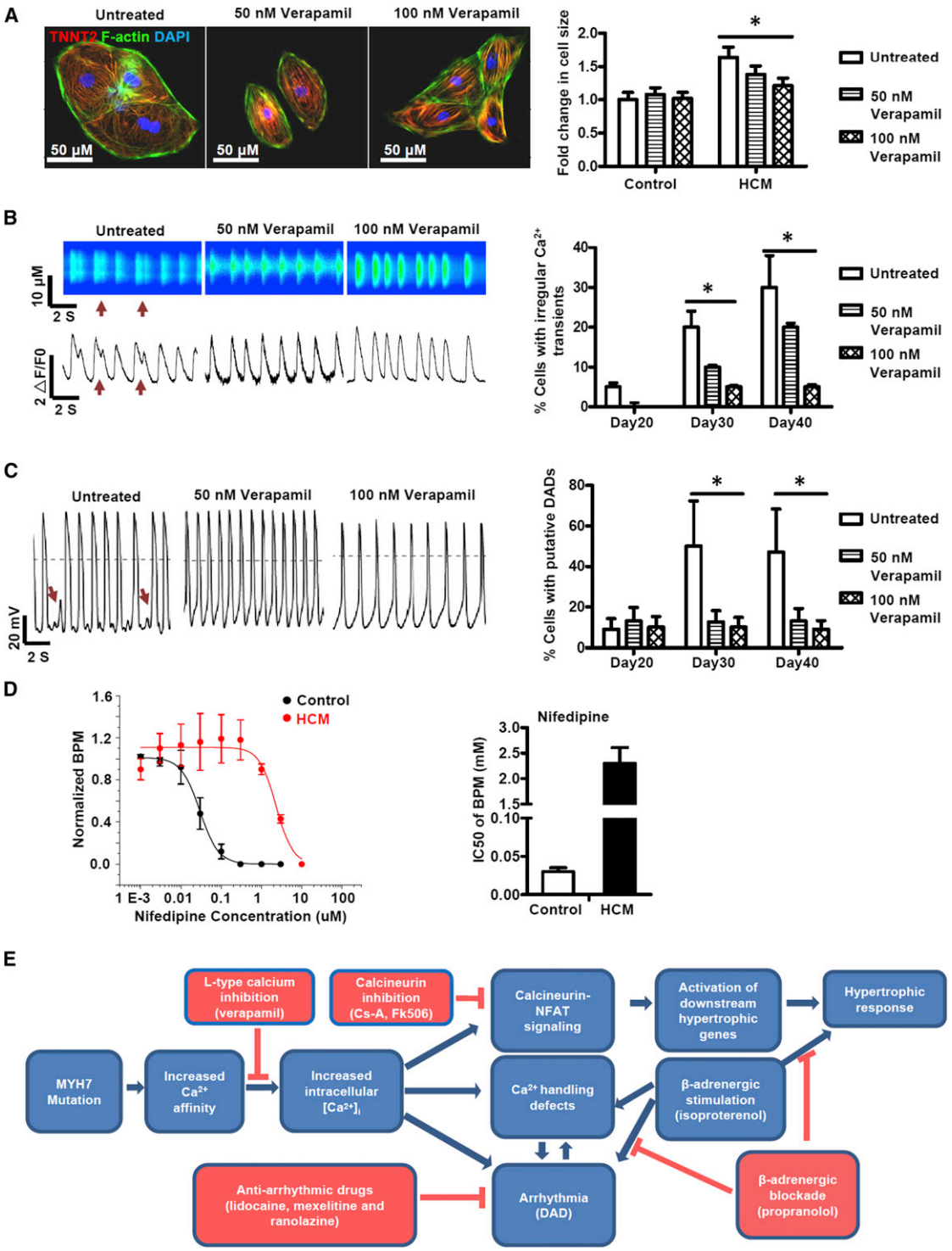

Figure 6. Treatment of HCM iPSC-CMs by Ca^{2+} Channel Inhibition Significantly Mitigates Development of the HCM Phenotype

(A) Representative immunostaining images of HCM iPSC-CMs treated with 0 nM, 50 nM, and 100 nM of the L-type Ca^{2+} channel blocker verapamil for 5 continuous days beginning 25 days after induction of cardiac differentiation. Quantification of relative cell sizes for HCM iPSC-CMs treated with verapamil (n = 50, 5 patient lines per treatment group).

(B) Representative Ca^{2+} line scan images and waveforms of HCM iPSC-CMs treated with 0 nM, 50 nM, and 100 nM of verapamil for 5 continuous days. Quantification of percentages of HCM iPSC-CMs found to exhibit irregular Ca^{2+} transients after treatment with verapamil (n = 40, 5 patient lines per treatment group).

(C) Representative electrophysiological recordings of spontaneous action potentials in HCM iPSC-CMs treated with 0 nM, 50 nM, and 100 nM of verapamil for 5 continuous days. Quantification of DAD frequencies in HCM iPSC-CMs after treatment with verapamil (n = 25, 5 patient lines per treatment group). See also Figures S5A–S5F.

(legend continued on next page)

α- or β-myosin isoforms. These issues and others have resulted in conflicting results for animal studies modeling HCM (Arad et al., 2002; Marian et al., 1997; Tyska et al., 2000).

Generation of patient-specific iPSC-CMs circumvents many of the limitations associated with transgenic animal models and has previously been used to model several hereditary cardiovascular disorders in vitro including dilated cardiomyopathy, LEOPARD, and long QT syndrome (Carvajal-Vergara et al., 2010; Itzhaki et al., 2011; Moretti et al., 2010; Narsinh et al., 2011a; Sun et al., 2012; Yazawa et al., 2011). To elucidate the mechanisms underlying HCM development, we utilized iPSC technology to generate functional cardiomyocytes from dermal fibroblasts of a ten-member family cohort, half of whom possess the HCM Arg663His mutation in the *MYH7* gene. Patient-specific iPSC-CMs recapitulated a number of characteristics of HCM including cellular hypertrophy, calcineurin-NFAT activation, upregulation of hypertrophic transcription factors, and contractile arrhythmia. Irregular Ca^{2+} transients and elevation of diastolic $[Ca^{2+}]_i$ were observed to precede the presentation of other phenotypic abnormalities, strongly implicating dysregulation of Ca^{2+} cycling as a central mechanism for pathogenesis of the disease.

Imbalances in Ca^{2+} homeostasis have been described as a key characteristic of HCM in numerous reports (Fatkin et al., 2000; Semsarian et al., 2002). However, little evidence exists to delineate whether these abnormalities are a symptom of HCM or a causal factor. In this study, we present several lines of evidence for a crucial role of Ca^{2+} in development of HCM as caused by the Arg663His mutation. Specifically, our findings suggest that an elevation in $[Ca^{2+}]_i$ mediated by the Arg663His mutation can induce both cellular hypertrophy and contractile arrhythmia (Figure 6E) (Fatkin and Graham, 2002). The sustained elevation of $[Ca^{2+}]_i$ is a known trigger for activation of calcineurin, a Ca^{2+}-dependent phosphatase that is a critical effector of hypertrophy in myocytes under conditions of stress. Activated calcineurin dephosphorylates *NFAT3* transcription factors, allowing their translocation to the nucleus for direct interaction with classical mediators of hypertrophy such as *GATA4* and *MEF2* (Molkentin et al., 1998; Sussman et al., 1998). Time-based gene expression profiling of single iPSC-CMs after induction of cardiac differentiation confirmed this model as expression of downstream effectors of hypertrophy was observed to be dependent on $[Ca^{2+}]_i$ elevation and nuclear translocation of NFAT. Inhibition of calcineurin activity by CsA and FK506 as well as reduction of Ca^{2+} influx by verapamil mitigated cellular hypertrophy, confirming the role of Ca^{2+} dysfunction and calcineurin-NFAT signaling in HCM pathogenesis.

Alterations in Ca^{2+} cycling are a common trigger for cardiac arrhythmias, which are a serious clinical complication of HCM due to their potential to induce stroke or sudden cardiac death (Bers, 2008). The mechanisms underlying arrhythmia in patients with HCM are not well understood, although reports have implicated interstitial fibrosis, abnormal cardiac anatomy, myocyte disarray, increased cell size, and dysfunction in Ca^{2+} homeostasis as possible mediators (Adabag et al., 2008; Wolf et al., 2005). Our findings demonstrate that the Arg663His mutation in the *MYH7* gene can directly result in electrophysiological and contractile arrhythmia at the single-cell level even in the absence of cellular hypertrophy. The most likely mechanism for development of arrhythmia in individual HCM iPSC-CMs is buildup of $[Ca^{2+}]_i$, which induces DADs, whereby sarcoplasmic reticulum Ca^{2+} release triggers transient inward current after action potential repolarization (Berlin et al., 1989; Bers, 2008; De Ferrari et al., 1995). Continued presentation of DADs can in turn lead to ventricular tachycardia and sudden cardiac death, as in patients suffering from recurrent arrhythmia (Iyer et al., 2007). Whole-cell current-clamp experiments of HCM iPSC-CMs supported this hypothesis through demonstration of frequent spontaneous DAD-like waveforms in diseased myocytes. We believe these results are the first report to demonstrate that HCM mutations such as Arg663His can act as direct triggers for arrhythmia at the single-cell level.

The hypothesis that dysfunction in Ca^{2+} homeostasis engenders the HCM phenotype was first proposed over a decade ago and is linked to the theory that HCM mutations increase myofilament Ca^{2+} affinity and cause "ion trapping" of Ca^{2+} in the cytoplasm (Fatkin et al., 2000; Semsarian et al., 2002). Although it is not entirely clear how the enhanced Ca^{2+} affinity would elevate free diastolic $[Ca^{2+}]_i$ as we have measured here, the mechanistic role of elevated myocyte Ca^{2+} loading seems to be central to both hypertrophy and arrhythmogenesis. Pharmaceutical drug screening of mutant iPSC-CMs further supported elevated $[Ca^{2+}]_i$ as a central mechanism for arrhythmia development. Of the 13 agents we used, only pharmaceutical blockade of Ca^{2+} and Na^+ entry mitigated contractile arrhythmia in HCM iPSC-CMs. Reduction of Na^+ influx limits $[Ca^{2+}]_i$ by allowing Na^+/Ca^{2+} exchange to remove Ca^{2+} more readily. Our results demonstrate the utility of iPSC-based technology to model development of HCM and associated triggered arrhythmias, as well as to identify potential therapeutic agents for the disease.

It is important to note that there are several limitations to our study. First, as described by several other reports, both hESC-CMs and iPSC-CMs are developmentally immature and are characterized by gene expression profiles similar to fetal cardiomyocytes, as well as lower levels of β-myosin than adult cardiomyocytes (Burridge et al., 2012; Cao et al., 2008; Carvajal-Vergara et al., 2010; Itzhaki et al., 2011). Second, iPSC-CMs are not able to model disease phenotypes that present at the tissue level such as interstitial fibrosis, scarring, and myocyte disarray. Finally, over 1,000 unique mutations have been identified to cause HCM, and our findings may only be specific to the Arg663His mutation. In spite of these limitations, we believe that our results are the first to provide direct evidence of elevation in $[Ca^{2+}]_i$ as an initiating factor in the development of HCM at the single-cell level. We anticipate that future studies utilizing

(D) Plots of average beat frequencies for control and HCM iPSC-CM EBs against nifedipine concentration fit to the Hill equation. Quantification of control and HCM IC_{50} values for spontaneous beat frequency against nifedipine (HCM, n = 8, 5 patient lines, control n = 13, 5 control subject lines).
(E) Schematic for development of the HCM phenotype as caused by HCM mutations in MYH7. Red boxes indicate potential methods to mitigate development of the disease. See also Figures S6A–S6E, Table S3, and Movie S3. *$p < 0.01$ untreated versus 50 nM verapamil versus 100 nM verapamil. **$p < 0.001$ HCM versus control. Error bars represent SEM.

disease-specific iPSC-CM models of HCM will focus on elucidation of how mutations in the thick filament cause Ca^{2+} handling defects as well as identification of alternative mechanisms underlying development of HCM.

EXPERIMENTAL PROCEDURES

Generation of Patient-Specific iPSCs

Protocols for this study were approved by the Stanford University Human Subjects Research Institutional Review Board and written consent was obtained from all study participants. Dermal fibroblasts were isolated from all family members and passaged three times before lentiviral infection with *OCT4*, *SOX2*, *KLF4*, and *c-MYC*. Colonies with iPSC morphology were lifted and maintained on Matrigel-coated plates (BD Biosciences) for maintenance with mTESR-1 growth medium (StemCell Technologies) as previously described (Sun et al., 2012).

Cardiac Differentiation of Patient-Specific iPSCs

Established iPSC lines from all subjects were differentiated into cardiomyocyte lineages (iPSC-CMs) using standard 3D EB differentiation protocols as previously described (Yang et al., 2008). For single cardiomyocyte analyses, beating EBs were plated on gelatin-coated dishes for 3 days, trypsinized, strained through a 40-mm-size pore-size filter, and replated as single cells on low density on gelatin-coated chamber slides (Nalgene Nunc International).

Ca^{2+} Imaging Using Fluo-4 AM

iPSC-CMs were dissociated from beating EBs and seeded in gelatin-coated 8-well LAB-TEK II chambers (Nalgene Nunc International). Cells were loaded with 5 μM Fluo-4 AM and imaged in Tyrodes solution using a confocal microscope (Carl Zeiss, LSM 510 Meta) at 40×. Spontaneous Ca^{2+} transients were recorded at 37°C using standard line-scan methods (Yazawa et al., 2011). A total of 10,000 line scans were acquired for durations of 19.2 s. For paced Ca^{2+} dye imaging, cells were stimulated at 1 and 2 Hz. Videos were taken at 20 fps for 10 s recording durations.

Patch Clamping

Whole-cell patch-clamp recordings were conducted on single beating cardiomyocytes at 36°C–37°C using an EPC-10 patch-clamp amplifier (HEKA) and a RC-26C recording chamber (Warner) mounted on to the stage of an inverted microscope (Nikon). Data were acquired using PatchMaster software (HEKA) and digitized at 1.0 kHz. Current-clamp recordings were conducted in Tyrodes solution.

Drug Treatment

Single contracting iPSC-CMs were treated with pharmaceutical agents for 10 min for immediate analysis followed by washout. The respective concentrations of each drug tested are listed in Table S3. For inotropic stimulation experiments, 200 nM isoproterenol and 400 nM propranolol were added to the cell medium for 5 continuous days. Verapamil treatment was conducted by adding 50 nM and 100 nM to the culture medium of iPSC-CMs for 10–20 continuous days on a daily basis.

Statistical Analysis

Statistical differences between two groups were determined using the two-tailed Student t tests. Statistical differences among more than two groups were analyzed by one-way ANOVA followed by Tukey's multiple comparison test. Denotation of a patient or control subject line is defined as one patient-specific line from one distinct individual.

A complete description of the methods is detailed in the Supplemental Experimental Procedures section.

SUPPLEMENTAL INFORMATION

Supplemental Information for this article includes six figures, three tables, Supplemental Experimental Procedures, and three movies and can be found with this article online at http://dx.doi.org/10.1016/j.stem.2012.10.010.

ACKNOWLEDGMENTS

We gratefully acknowledge funding support from Burroughs Wellcome Foundation, Foundation Ledvcq, NIH New Innovator Award DP2OD004437, R01 HL113006 CIRM RB3-05129 (J.C.W.), RC1 HL100490 (M.T.L.), HHMI (A.S.L.), Bio-X (A.S.L.), and U01 HL099776 (R.C.R.).

Received: April 27, 2012
Revised: August 16, 2012
Accepted: October 12, 2012
Published: January 2, 2013

REFERENCES

Adabag, A.S., Maron, B.J., Appelbaum, E., Harrigan, C.J., Buros, J.L., Gibson, C.M., Lesser, J.R., Hanna, C.A., Udelson, J.E., Manning, W.J., and Maron, M.S. (2008). Occurrence and frequency of arrhythmias in hypertrophic cardiomyopathy in relation to delayed enhancement on cardiovascular magnetic resonance. J. Am. Coll. Cardiol. *51*, 1369–1374.

Arad, M., Seidman, J.G., and Seidman, C.E. (2002). Phenotypic diversity in hypertrophic cardiomyopathy. Hum. Mol. Genet. *11*, 2499–2506.

Berlin, J.R., Cannell, M.B., and Lederer, W.J. (1989). Cellular origins of the transient inward current in cardiac myocytes. Role of fluctuations and waves of elevated intracellular calcium. Circ. Res. *65*, 115–126.

Bers, D.M. (2008). Calcium cycling and signaling in cardiac myocytes. Annu. Rev. Physiol. *70*, 23–49.

Burridge, P.W., Keller, G., Gold, J.D., and Wu, J.C. (2012). Production of de novo cardiomyocytes: human pluripotent stem cell differentiation and direct reprogramming. Cell Stem Cell *10*, 16–28.

Cao, F., Wagner, R.A., Wilson, K.D., Xie, X., Fu, J.D., Drukker, M., Lee, A., Li, R.A., Gambhir, S.S., Weissman, I.L., et al. (2008). Transcriptional and functional profiling of human embryonic stem cell-derived cardiomyocytes. PLoS One *3*, e3474.

Carvajal-Vergara, X., Sevilla, A., D'Souza, S.L., Ang, Y.S., Schaniel, C., Lee, D.F., Yang, L., Kaplan, A.D., Adler, E.D., Rozov, R., et al. (2010). Patient-specific induced pluripotent stem-cell-derived models of LEOPARD syndrome. Nature *465*, 808–812.

De Ferrari, G.M., Viola, M.C., D'Amato, E., Antolini, R., and Forti, S. (1995). Distinct patterns of calcium transients during early and delayed afterdepolarizations induced by isoproterenol in ventricular myocytes. Circulation *91*, 2510–2515.

Fatkin, D., and Graham, R.M. (2002). Molecular mechanisms of inherited cardiomyopathies. Physiol. Rev. *82*, 945–980.

Fatkin, D., Christe, M.E., Aristizabal, O., McConnell, B.K., Srinivasan, S., Schoen, F.J., Seidman, C.E., Turnbull, D.H., and Seidman, J.G. (1999). Neonatal cardiomyopathy in mice homozygous for the Arg403Gln mutation in the alpha cardiac myosin heavy chain gene. J. Clin. Invest. *103*, 147–153.

Fatkin, D., McConnell, B.K., Mudd, J.O., Semsarian, C., Moskowitz, I.G., Schoen, F.J., Giewat, M., Seidman, C.E., and Seidman, J.G. (2000). An abnormal Ca(2+) response in mutant sarcomere protein-mediated familial hypertrophic cardiomyopathy. J. Clin. Invest. *106*, 1351–1359.

Geisterfer-Lowrance, A.A., Kass, S., Tanigawa, G., Vosberg, H.P., McKenna, W., Seidman, C.E., and Seidman, J.G. (1990). A molecular basis for familial hypertrophic cardiomyopathy: a beta cardiac myosin heavy chain gene missense mutation. Cell *62*, 999–1006.

Gruver, E.J., Fatkin, D., Dodds, G.A., Kisslo, J., Maron, B.J., Seidman, J.G., and Seidman, C.E. (1999). Familial hypertrophic cardiomyopathy and atrial fibrillation caused by Arg663His beta-cardiac myosin heavy chain mutation. Am. J. Cardiol. *83*(12A), 13H–18H.

Hossain, M.M., Shimizu, E., Saito, M., Rao, S.R., Yamaguchi, Y., and Tamiya, E. (2010). Non-invasive characterization of mouse embryonic stem cell derived cardiomyocytes based on the intensity variation in digital beating video. Analyst (Lond.) *135*, 1624–1630.

Itzhaki, I., Maizels, L., Huber, I., Zwi-Dantsis, L., Caspi, O., Winterstern, A., Feldman, O., Gepstein, A., Arbel, G., Hammerman, H., et al. (2011).

Modelling the long QT syndrome with induced pluripotent stem cells. Nature *471*, 225–229.

Iyer, V., Hajjar, R.J., and Armoundas, A.A. (2007). Mechanisms of abnormal calcium homeostasis in mutations responsible for catecholaminergic polymorphic ventricular tachycardia. Circ. Res. *100*, e22–e31.

Knollmann, B.C., Kirchhof, P., Sirenko, S.G., Degen, H., Greene, A.E., Schober, T., Mackow, J.C., Fabritz, L., Potter, J.D., and Morad, M. (2003). Familial hypertrophic cardiomyopathy-linked mutant troponin T causes stress-induced ventricular tachycardia and Ca2+-dependent action potential remodeling. Circ. Res. *92*, 428–436.

Lompre, A.M., Mercadier, J.J., Wisnewsky, C., Bouveret, P., Pantaloni, C., D'Albis, A., and Schwartz, K. (1981). Species- and age-dependent changes in the relative amounts of cardiac myosin isoenzymes in mammals. Dev. Biol. *84*, 286–290.

Lowey, S., Lesko, L.M., Rovner, A.S., Hodges, A.R., White, S.L., Low, R.B., Rincon, M., Gulick, J., and Robbins, J. (2008). Functional effects of the hypertrophic cardiomyopathy R403Q mutation are different in an alpha- or beta-myosin heavy chain backbone. J. Biol. Chem. *283*, 20579–20589.

Marian, A.J., Zhao, G., Seta, Y., Roberts, R., and Yu, Q.T. (1997). Expression of a mutant (Arg92Gln) human cardiac troponin T, known to cause hypertrophic cardiomyopathy, impairs adult cardiac myocyte contractility. Circ. Res. *81*, 76–85.

Maron, B.J. (2002). Hypertrophic cardiomyopathy: a systematic review. JAMA *287*, 1308–1320.

Maron, B.J., Gardin, J.M., Flack, J.M., Gidding, S.S., Kurosaki, T.T., and Bild, D.E. (1995). Prevalence of hypertrophic cardiomyopathy in a general population of young adults. Echocardiographic analysis of 4111 subjects in the CARDIA Study. Coronary Artery Risk Development in (Young) Adults. Circulation *92*, 785–789.

Maron, B.J., Shirani, J., Poliac, L.C., Mathenge, R., Roberts, W.C., and Mueller, F.O. (1996). Sudden death in young competitive athletes. Clinical, demographic, and pathological profiles. JAMA *276*, 199–204.

Maron, M.S., Olivotto, I., Betocchi, S., Casey, S.A., Lesser, J.R., Losi, M.A., Cecchi, F., and Maron, B.J. (2003). Effect of left ventricular outflow tract obstruction on clinical outcome in hypertrophic cardiomyopathy. N. Engl. J. Med. *348*, 295–303.

Molkentin, J.D., Lu, J.R., Antos, C.L., Markham, B., Richardson, J., Robbins, J., Grant, S.R., and Olson, E.N. (1998). A calcineurin-dependent transcriptional pathway for cardiac hypertrophy. Cell *93*, 215–228.

Moretti, A., Bellin, M., Welling, A., Jung, C.B., Lam, J.T., Bott-Flügel, L., Dorn, T., Goedel, A., Höhnke, C., Hofmann, F., et al. (2010). Patient-specific induced pluripotent stem-cell models for long-QT syndrome. N. Engl. J. Med. *363*, 1397–1409.

Narsinh, K., Narsinh, K.H., and Wu, J.C. (2011a). Derivation of human induced pluripotent stem cells for cardiovascular disease modeling. Circ. Res. *108*, 1146–1156.

Narsinh, K.H., Sun, N., Sanchez-Freire, V., Lee, A.S., Almeida, P., Hu, S., Jan, T., Wilson, K.D., Leong, D., Rosenberg, J., et al. (2011b). Single cell transcriptional profiling reveals heterogeneity of human induced pluripotent stem cells. J. Clin. Invest. *121*, 1217–1221.

Seidman, J.G., and Seidman, C. (2001). The genetic basis for cardiomyopathy: from mutation identification to mechanistic paradigms. Cell *104*, 557–567.

Semsarian, C., Ahmad, I., Giewat, M., Georgakopoulos, D., Schmitt, J.P., McConnell, B.K., Reiken, S., Mende, U., Marks, A.R., Kass, D.A., et al. (2002). The L-type calcium channel inhibitor diltiazem prevents cardiomyopathy in a mouse model. J. Clin. Invest. *109*, 1013–1020.

Sun, N., Yazawa, M., Liu, J., Han, L., Sanchez-Freire, V., Abilez, O.J., Navarrete, E.G., Hu, S., Wang, L., Lee, A., et al. (2012). Patient-specific induced pluripotent stem cells as a model for familial dilated cardiomyopathy. Sci. Transl. Med. *4*, 130ra147.

Sussman, M.A., Lim, H.W., Gude, N., Taigen, T., Olson, E.N., Robbins, J., Colbert, M.C., Gualberto, A., Wieczorek, D.F., and Molkentin, J.D. (1998). Prevention of cardiac hypertrophy in mice by calcineurin inhibition. Science *281*, 1690–1693.

Teare, D. (1958). Asymmetrical hypertrophy of the heart in young adults. Br. Heart J. *20*, 1–8.

Tyska, M.J., Hayes, E., Giewat, M., Seidman, C.E., Seidman, J.G., and Warshaw, D.M. (2000). Single-molecule mechanics of R403Q cardiac myosin isolated from the mouse model of familial hypertrophic cardiomyopathy. Circ. Res. *86*, 737–744.

Wolf, C.M., Moskowitz, I.P., Arno, S., Branco, D.M., Semsarian, C., Bernstein, S.A., Peterson, M., Maida, M., Morley, G.E., Fishman, G., et al. (2005). Somatic events modify hypertrophic cardiomyopathy pathology and link hypertrophy to arrhythmia. Proc. Natl. Acad. Sci. USA *102*, 18123–18128.

Yang, L., Soonpaa, M.H., Adler, E.D., Roepke, T.K., Kattman, S.J., Kennedy, M., Henckaerts, E., Bonham, K., Abbott, G.W., Linden, R.M., et al. (2008). Human cardiovascular progenitor cells develop from a KDR+ embryonic-stem-cell-derived population. Nature *453*, 524–528.

Yazawa, M., Hsueh, B., Jia, X., Pasca, A.M., Bernstein, J.A., Hallmayer, J., and Dolmetsch, R.E. (2011). Using induced pluripotent stem cells to investigate cardiac phenotypes in Timothy syndrome. Nature *471*, 230–234.